Journal of Materials Chemistry A

Accepted Manuscript

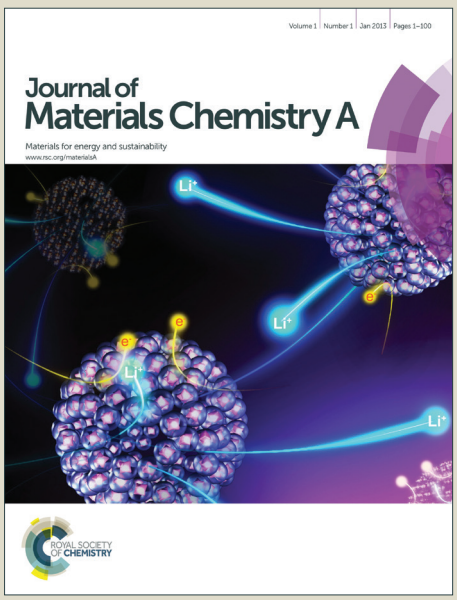

ROYAL SOCIETY OF CHEMISTRY

www.rsc.org/materialsA

Cite this: DOI: 10.1039/c0xx00000x

www.rsc.org/xxxxxx

ARTICLE TYPE

Nanoconfinement of phase change materials within Carbon Aerogels: Phase Transition Behaviours and Photo-to-Thermal Energy Storage

Xinyu Huang, Wei Xia, and Ruqiang Zou*

Received (in XXX, XXX) Xth XXXXXXXXX 20XX, Accepted Xth XXXXXXXXX 20XX

DOI: 10.1039/b000000x

We systematically investigate the thermal energy storage property and host-guest interactions in a phase change composite based on octadecanol/carbon aerogels. Due to the nanoconfinement effect induced by the carbon aerogels, the loaded active materials show distinct phase transition behaviour to the free octadecanol, in which the solid-to-solid and solid-to-liquid phase change process occurred at a lower temperature and the interval between these two process became larger.

Introduction

The mismatch between the energy supply and demand during energy conversing and delivering is a critical problem in the current industry field.[1-3] As energy storage system being an answer to the problem, latent heat storage system using phase change materials (PCMs) can significantly increase the efficiency of the system.[1, 3-6] Phase change materials can store large amount of energy at a constant temperature.[5, 7-9] The relatively stable property and low price also make PCMs attractive and suitable for off-peak electricity storage as well as for building.[5, 7, 10-14] Among the large number of phase change materials, organic PCMs have been thoroughly investigated for the large range of practical melting point and a moderate thermal storage density.[8, 15-27] Furthermore, the volume changes of organic PCMs are indistinctive when the phase change occurs, which causes less fracture to the container. However, one factor hindering organic PCMs from practical application is the leakage of liquid-state PCMs.[28-29] Methods like micro-capsulation[20, 30-31] and electrospun[32-38] have been developed to solve the problem. More recently, loading PCM into porous media to prevent leakage has shown great potential.

Porous materials have been thoroughly studied owing to the excellent natures such as large surface area, pore volume and low density. Based on the properties, porous materials can be applied in sensors,[39] gas separation,[40] drug delivery,[41] batteries,[42] catalysts,[43] as well as phase change materials.[44-45] Porous materials can hold PCMs in the pores by capillarity, which makes them an excellent substrate for phase change material encapsulation. They also show the advantages in flexible shape and steady property.[46-48] Various porous materials have been used to encapsulate PCMs. For example, SBA-15,[49] Al foam,[50] carbon foam,[51] carbon nanotube,[52] carbon nanotube sponge[53] or expanded graphite[54-55] have been applied to make phase change composites. To ensure the largest PCM loading ratio in the composite, carbon-based material is the optimal substrate because of its low density and high porosity. Porous carbon materials provide ultrahigh specific surface area which keeps the PCM in situ by surface tension. Advanced porous carbon material like graphene aerogel has been used to form phase change composite with octadecanoic acid loading[56] and it showed a similar high heat storage capacity but much enhanced thermal conductivity to pure octadecanoic acid. Despite tremendous work showing how much porous carbon substrates can improve the heat storage capacity and the additional benefits of preventing corrosion and agglomeration, a further question on how these carbon substrates can affect the phase change materials at molecular level during phase change process is unclear.

Here we fabricated a carbon aerogel/octadecanol phase change composite and we found apparently different phase change behaviour in the composite to pure octadecanol, which was not reported before.[57-58] When octadecanol was infiltrated into this carbon aerogel, the phase change process was influenced due to the disturbance of the aerogel on the crystal structure of PCM, which implied a novel strategy for altering the phase change temperature of PCM. The phase change composite was systematically studied to disclose the host-guest interaction in the aerogel/octadecanol system. Moreover, we realized an energy transfer from light to thermal with this phase change composite.

Experimental

Synthesis

The carbon aerogel was synthesized from glucose based on the reported method.[59] 473.47 mg disodium tetraborate decahydrate ($Na_2B_4O_7{\cdot}10H_2O$) and 6.5 g D-glucose were dissolved in 15 ml deionized water through stirring to get a uniform solution. The solution was transferred into quartz tubes and sealed in a Teflon-lined reactor which was then heated at 180 °C for 8 hours. The as-prepared products were immersed in ethanol several times to remove the remaining reactant and exchange water to ethanol.[60] The gels were dried by supercritical CO_2 afterwards, then carbonized under Ar atmosphere at 550°C for 5 h with a heating rate of 10 K/min. Then the carbon aerogel was immersed either into pure octadecanol or octadecanol-ethanol homogenous solution at the temperature of 80 °C, so as to obtain samples with different octadecanol loading.[61] After that, they were dried in a vacuum oven at 80°C.

Characterization

Differential scanning calorimeter (Setaram DSC 131 evo) measurements were conducted under the protection of Ar. All the samples with weights between 3 to 5mg were placed in an Al 30 μL pan. The temperature change rate of the instrument was 5 °C/min. Thermo-gravimetric analysis (TGA) data were obtained on a thermo-gravimetric analysis instrument (TA-SDT-Q600) under the protection of N_2 at a heating rate of 10 °C/min and the sample weights were between 1 and 5 mg. Scanning electron microscopy (SEM) characterization was performed using a field-emission microscope (Hitachi-S4800) operated at 10 kV. The X-ray photoelectron spectroscopy (XPS) data were taken from an AXIS Ultra instrument from Kratos Analytical. The data were converted into VAMAS file format and imported into CasaXPS software package for manipulation and curve-fitting. X-ray diffraction (XRD) experiments were performed using a Japan DMAX-2400 in the range of 0°-50°. High-energy X-ray diffraction was employed to study the intermolecular interaction at the 11-ID-C beam line at the Advanced Photon Source at Argonne National Laboratory. Photo-to-thermal energy conversion test was carried out by using a Newport Thermo Oriel 91195A-1000 solar simulator. Sample temperature was recorded by a RKC hand held digital thermometer DP-700 data collector.

Results and Discussion

The phase change composite was obtained by immersing the aerogel into melted octadecanol or octadecanol solution. Because of the hydrophobic nature of the aerogel, melted octadecanol can easily be impregnated in it. A rough fraction between carbon aerogel and octadecanol was first determined by the mass difference of the initial aerogel and the composite after the infiltration. Four carbon aerogel-octadecanol samples are synthesized and marked as composite-1(C1), composite-2(C2) composite-3(C3) and composite-4(C4), with rough octadecanol mass fraction of 76%, 68%, 60%, and 48%, respectively. Element analysis was performed by XPS (Figure S3). The result shows that carbon and oxygen are the two main elements in the aerogel, with atom percentage of 92.76% and 6.98%, respectively. XPS result reveals the absence of boron or sodium in the aerogel, which indicates that catalyst has been wiped out during the solvent exchange.

SEM images of the pure carbon aerogel and the composite are displayed in Figure 1c-f. The aerogel assembled from the interconnected nanoparticles are highly porous with a high degree of macro-porosity, which fulfilled the infiltration of PCM. The microstructure of the carbon aerogel was further revealed by nitrogen sorption experiment. Figure 2a displays the sorption isotherms for carbon aerogel and the PCM composite. For pure carbon aerogel, it has Type-II isotherms revealing the presence of micro-porosity as well as macro-porosity. More details can be found in its corresponding pore size distribution (PSD) that shows a wide pore distribution from micro-pores to meso-pores. After PCM infiltration, the sample showed a denser structure (Figure 1e-f). The rough nanoparticles were filled and wrapped by phase change material, which lead to the observed smooth surface. The capillary between the aerogel and octadecanol can prevent the octadecanol from leakage at temperature above the melting points of PCM. The filling of the octadecanol in the porous aerogel can be further verified by the sharply decreased nitrogen sorption capacity and the disappearance of pores from PSD.

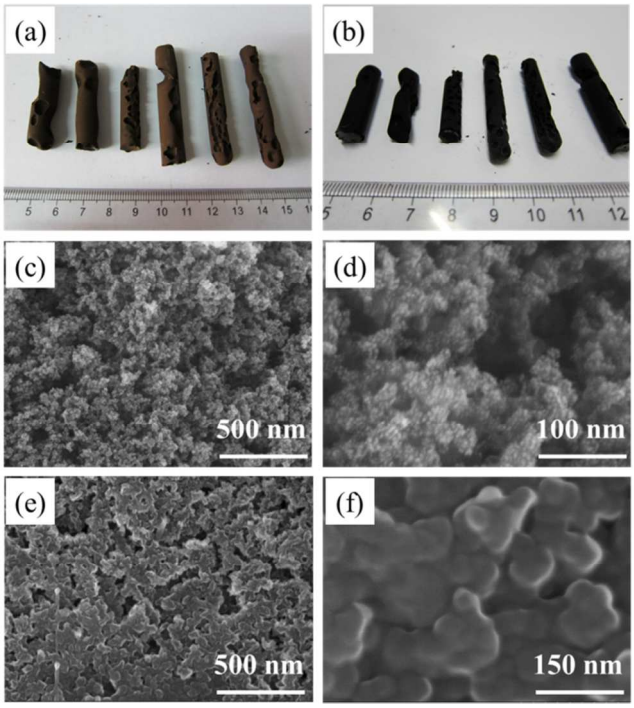

Fig. 1 View of the carbon aerogel and the octadecanol@carbon aerogel composites. (a) the optical photo of carbon aerogel before carbonization, (b) the optical photo of carbon aerogel after carbonization, (c,d) SEM images of the carbon aerogel with different magnifications, and (e,f) SEM images of C1 with corresponding magnification.

To disclose the mutual effect between oxygen-doping substrate and octadecanol, XRD measurements on samples with different octadecanol contents had been carried out, as illustrated in Figure 2b. The bottom pattern in black color is the simulated XRD curve of octadecanol, and the pattern of pure octadecanol in red colour fits well with it. Comparing the patterns of pure octadecanol and C1, an obvious peak shift to lower degree at about 5° should be noticed. The shift results from the unit cell expansion of octadecanol, which could have an effect on its phase change process. No evident peak appears at low degree in pattern of C3 and C4, blocked by the pattern of amorphous aerogel.

TGA had been performed to study the thermal stability of the composite and determined the accurate loading percentage of octadecanol in the composite, showed in Figure 3a. Each specimen came out of the inner part of every composite for TGA measurement. The TGA curves show that the carbon-based aerogel loses little weight with temperature rising, while octadecanol is thermally decomposed at about 200 °C. After octadecanol infiltrated into the aerogel, the composite shows a weight reduction at a higher temperature around 250 °C followed by a platform of residual substrate. The aerogel makes contribution to the thermal stability of the composite because of the interaction between the aerogel and octadecanol. The exact fraction of the octadecanol immersed in the composite had been confirmed by TGA test, and the ratios of octadecanol in C1, C2, C3 and C4 were modified as 75.9%, 71.1%, 50.0% and 44.3%.

The results indicated that there is little difference between rough calculation and exact fraction.

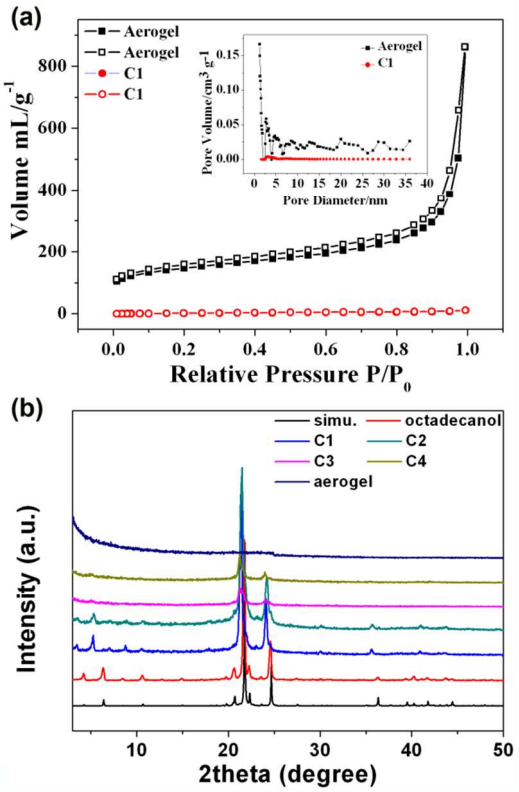

Fig. 2 N_2 absorption and desorption isotherms of the carbon aerogel and C1, inset shows the corresponding pore distributions. (b) XRD pattern of the octadecanol, carbon aerogel and C1 to C4. Details from 20° to 25° are depicted in the inset.

The thermal behavior of the composites was studied by the differential scanning calorimetry (DSC). The comparison between pure octadecanol and sample C1 (Figure 3b& Figure S1) indicates a disruption of the phase change process as the caloric peaks show a different pattern from the original one: the one peak during endothermic process is replaced by two peak, while the distance between the original two peaks during exothermic process is larger. This phenomenon suggests a novel interaction between the organic molecules and the carbon material, which is explained in the following paragraphs. Detailed enthalpy comparison of the samples are showed in Table S1. The ratio between infiltration percentage and weight percentage indicated an effect of the support material on the motion of the octadecanol.[61] The thermal stability of the PCM-carbon aerogel composite can be illustrated by the 50 cycle test of C2 and the 10 cycle test of C1 as shown in Figure 3c and 3d. The cycled DSC patterns fit well with one another, reflecting the good cycle performance of the composite through circulation.

The crystal structure of octadecanol is illustrated in Figure 4a. Red lines represent the hydrogen bonding in the crystal. According to the crystal structures analysis of n-alkanols reported previously, [62] octadecanol has a monoclinic γ-phase, containing eight molecules in the unit cell, at room temperature. The hydrogen bonds between octadecanol links are parallel to (*100*) plane. In the composites, the ordinary order of the octadecanol molecule is interrupted by the amorphous carbon aerogel, whereas, the effect can be treated as the PCM crystal unit cell is enlarged. Larger distance between adjacent octadecanol molecules rendered a loosened nonpolar interaction between methyl groups and weaken hydrogen bonding (Figure S2), leading to a less compacted molecular array. Therefore, the rotation of the hydrocarbon chain requires lower thermal energy, resulting in a solid-solid phase transition occurring 2-3 °C in advance. The phase change separation caused by the unit cell enlargement can also be observed during the exothermic process. A large separation about 10 °C was observed. The details of the crystal structure switch are verified by high-energy X-ray diffraction of C1 (Figure 4b, 4c). Simplified radical distribution function G(r) is used to describe the structure of non-crystalline phase based on statistical physics. The pattern taken at 70 °C, which was beyond the melting point, shows an obvious difference from others because the octadecanol transforms into liquid phase and the organic molecules are in a homogeneous state. The detailed radical distribution function from 1 to 10 angstrom illustrates the inter-molecule distance change at different temperatures, as shown in Figure 6c. A peak arises when the temperature rose from 30 °C to 60 °C at r= 2.18Å, and dismissed at 70 °C. The corresponding change in molecular structure is the solid-solid phase change resulting from the rotation of the hydrocarbon chain. This could also be verified by the peaks at r= 2.5 Å. The patterns of 30 °C and 50 °C fit with that of 40 °C and 60 °C, respectively, while the latter group has a higher peak height and the 70 °C pattern is the highest. These three series is ascribed to the γ, β and liquid phase. We have employed carbon nanotube to accomplish high proportion phase change composite for thermal energy storage.[53, 63] However, the effect on the crystallization of the PCM from the host was not observed. Here, the temperature shifts are due to the disturbance of the PCM's crystalline structure and the pores in the aerogel are mainly micropores and mesopores. So the interaction between the PCM and porous framework would be strong enough to disturb its phase change process when the pore can confine the crystallization of the PCM. This could be the reason why this phenomenon was not observed before.

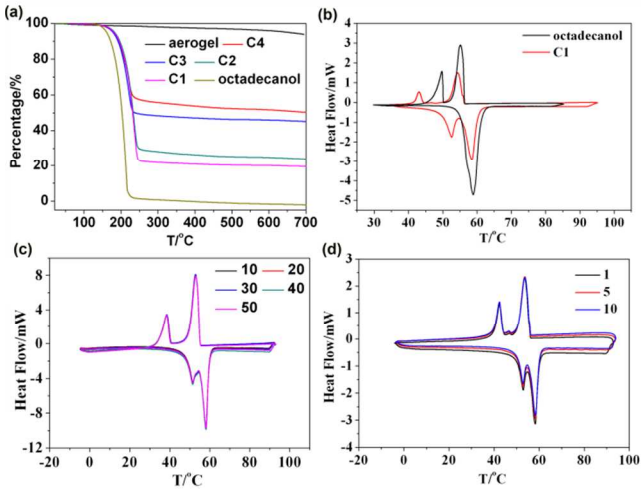

Fig. 3 Thermal properties of the phase change composites. (a) TGA curves of the aerogel, octadecanol and composites. (b) The DSC results comparison between pure octadecanol and C1. (c,d) reveal 50 and 10 DSC cycles test of C2 and C1, respectively.

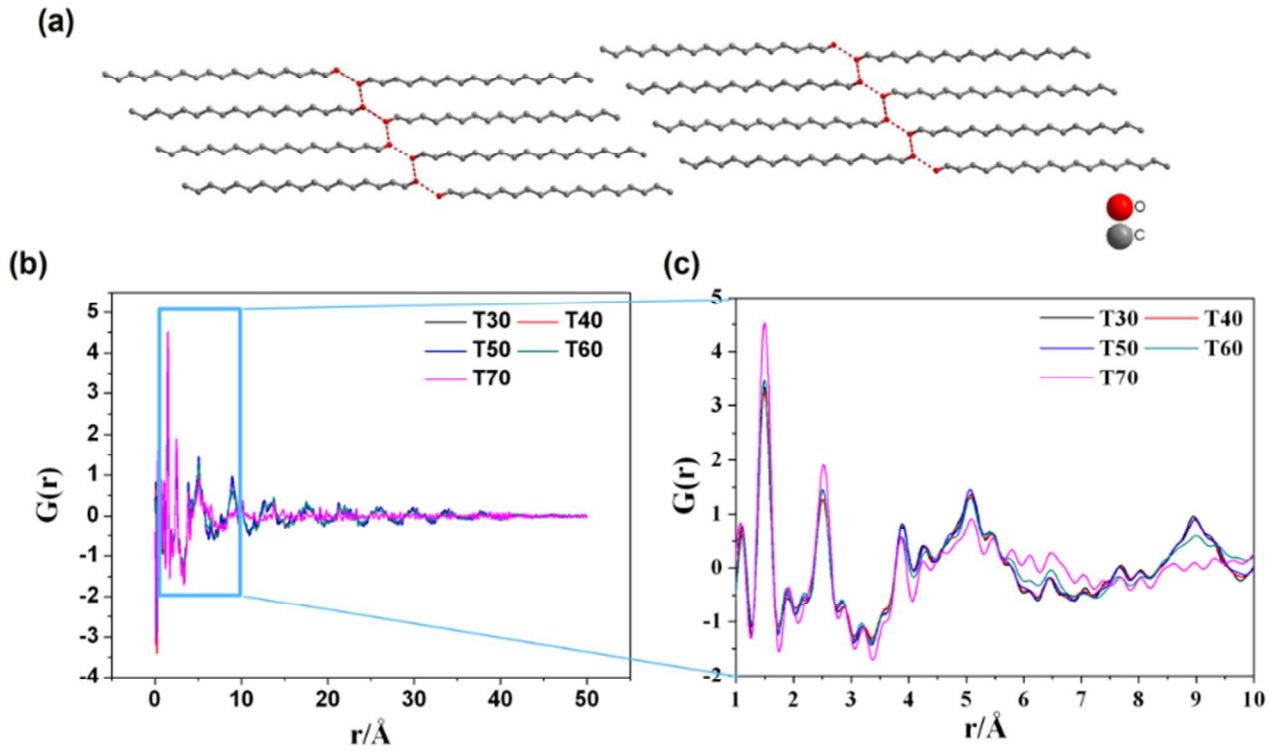

Fig. 4 Phase change behavior of octadecanol in the composite. (a) The crystal structure illustration of octadecanol. Red lines indicate the hydrogen bonding between molecules. (b) The PDF curves of phase change of C1. (c) Detail of the PDF curves ranging from r=1 Å to r=10 Å, giving the very particular structure changes when temperature rises.

The black appearance of the composite rendered it an ideal light absorbent. The light-to-heat energy conversion measurement is illustrated in Figure 5a. The composite was placed under the simulated solar radiation with an intensity of 100mW/cm^2. During the light radiation, the composite can absorb solar energy and its temperature rose. When the temperature reached the melting point of octadecanol, an inflection point appears in the temperature change curve, which indicates the phase change process takes place. However, only one phase change process can be distinguished from the plot during the temperature rising of the composite which made the difference between two phase change temperatures less noticeable. The highest temperature of light-to-heat conversion can be 62.2 °C and the temperature platform owed the balance of the absorbed light energy and the dispersed heat to the air. Two temperature platforms can be easily observed which mean phase change processes after the light was removed and the temperature decreases. If the intensity was reduced to 50 mW/cm^2, the highest temperature was 48.5 °C, without a phase change phenomenon. A sample of pure octadecanol is also tested under the light of 100mW/cm^2, and its pattern is more similar to that of the composite under a light of half intensity. The pure octadecanol had a white surface and it would reflect the irradiated light, which means that the temperature of the octadecanol can't reach its melting point and realize the solar energy storage. Compared to the pure octadecanol, the phase change composite based on carbon aerogel had better performance in photo-energy absorption and form-stability (Figure S4, S5).

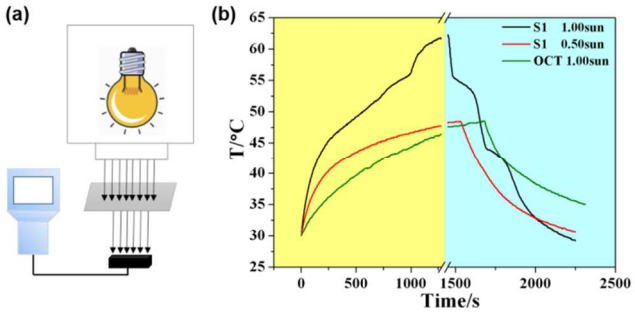

Fig. 5 Photo-to-thermal transfer of the composite under different light intensity: (a) Illustration of the photo-to-thermal energy conversion and (b) The time-temperature curves of the octadecanol and phase change composites.

Conclusions

In summary, the phase transition mechanism of the octadecanol encapsulated in a glucose-derived carbon aerogel was discussed in our work. The regular molecule array of the octadecanol is disturbed by the amorphous carbon aerogel, which results in the phase transition temperature occurring at a lower temperature. In addition, the molecular distance enlargement also separates the solid-solid and solid-liquid phase change processes. We have also realized photo-to-thermal energy conversion using the phase change composite for the practical application in thermal energy storage. The composite showed a high energy capacity than pure phase change material and could reach a temperature as high as 62.2 °C. Our work suggests a new approach to study the phase

change behaviour of phase change composite and provide a composite for solar-to-thermal energy storage.

Acknowledgements

This work was supported by National Natural Science Foundation of China 51322205 and 21371014, New Star Program of Beijing Committee of Science and Technology (2012004) and the Ministry of education program for New Century Excellent Talents of China (NCET-11-0027).

Notes and references

Department of Materials Science and Engineering, College of Engineering, Peking University, Beijing P. R. China, 100871.
Email: rzou@pku.edu.cn

† Electronic Supplementary Information (ESI) available: [for the DSC result of pure octadecanol; and the IR spectra of the composite, pure octadecanol]. See DOI: 10.1039/b000000x/

1. A. M. Khudhair and M. M. Farid, *Energy Convers. Manag.*, 2004, **45**, 263-275.
2. M. M. Farid, A. M. Khudhair, S. A. K. Razack and S. Al-Hallaj, *Energy Convers. Manag.*, 2004, **45**, 1597-1615.
3. B. Cárdenas and N. León, *Renew Sustain Energy Rev*, 2013, **27**, 724-737.
4. A. Sharma, V. V. Tyagi, C. R. Chen and D. Buddhi, *Renew Sustain Energy Rev*, 2009, **13**, 318-345.
5. B. Zalba, J. M. Marin, L. F. Cabeza and H. Mehling, *Appl. Therm. Eng.*, 2003, **23**, 251-283.
6. E. Oró, A. de Gracia, A. Castell, M. M. Farid and L. F. Cabeza, *Appl. Energy*, 2012, **99**, 513-533.
7. Y. Wang, B. Tang and S. Zhang, *J. Mater. Chem.*, 2012, **22**, 18145-18150.
8. N. Sarier and E. Onder, *Thermochim. Acta*, 2012, **540**, 7-60.
9. Y. Li, Z. Y. Fu and B. L. Su, *Adv. Funct. Mater.*, 2012, **22**, 4634-4667.
10. T. C. Ling and C. S. Poon, *Constr. Build. Mater.*, 2013, **46**, 55-62.
11. D. G. L. Samuel, S. M. S. Nagendra and M. P. Maiya, *Build. Envir.*, 2013, **66**, 54-64.
12. S. Marchi, S. Pagliolico and G. Sassi, *Energy Convers. Manag.*, 2013, **74**, 261-268.
13. L. F. Cabeza, A. Castell, C. Barreneche, A. de Gracia and A. I. Fernández, *Renew Sustain Energy Rev*, 2011, **15**, 1675-1695.
14. M. Jradi, M. Gillott and S. Riffat, *Appl. Therm. Eng.*, 2013, **59**, 211-222.
15. H. Li, M. Jiang, Q. Li, D. Li, Z. Chen, W. Hu, J. Huang, X. Xu, L. Dong, H. Xie and C. Xiong, *Energy Convers. Manag.*, 2013, **75**, 482-487.
16. T. Y. Wang and J. Huang, *J. Appl. Polym. Sci.*, 2013, **130**, 1516-1523.
17. A. Sari, *Energy Convers. Manag.*, 2012, **64**, 68-78.
18. C. Y. Wang, L. L. Feng, H. Z. Yang, G. B. Xin and Wei Li, *Phys. Chem. Chem. Phys.*, 2012, **14**, 13233-13238.
19. F. Yavari, H. R. Fard, K. Pashayi, M. A. Rafiee, A. Zamiri, Z. Yu, R. Ozisik, T. Borca-Tasciuc and N. Koratkar, *J. Phys. Chem. C*, 2011, **115**, 8753-8758.
20. L. Pan, Q. Tao, S. Zhang, S. Wang, J. Zhang, S. Wang, Z. Wang and Z. Zhang, *Sol. Energy Mater. Sol. Cells*, 2012, **98**, 66-70.
21. L. Pan, Q. Ji, Y. Qin, Y. Jiang, Z. Zhang, S. Zhang and Z. Wang, *RSC Adv.*, 2013, 3, 22326-22331.
22. M. Li, Z. Wu, H. Kao and J. Tan, *Energy Convers. Manag.*, 2011, **52**, 3275-3281.
23. J. Wang, H. Xie, Z. Xin, Y. Li and L. Chen, *Sol. Energy*, 2010, **84**, 339-344.
24. A. Sari and A. Bicer, *Sol. Energy Mater. Sol. Cells*, 2012, **101**, 114-122.
25. A. A. Aydin and A. Aydin, *Sol. Energy Mater. Sol. Cells*, 2012, **96**, 93-100.
26. H. Kao, M. Li, X. Lv and J. Tan, *J Therm Anal Calorim*, 2012, **107**, 299-303.
27. K. Chintakrinda, R. D. Weinstein and A. S. Fleischer, *Int J Therm Sci*, 2011, **50**, 1639-1647.
28. T. Nomura, N. Okinaka and T. Akiyama, *Mater. Chem. Phys.*, 2009, **115**, 846-850.
29. W. Hu and X. Yu, *RSC Adv.*, 2012, **2**, 5580-5584.
30. W. Li, G. Song, G. Tang, X. Chu, S. Ma and C. Liu, *Energy*, 2011, **36**, 785-791.
31. C. Alkan, A. Sari and A. Karaipekli, *Energy Convers. Manag.*, 2011, **52**, 687-692.
32. Y. Cai, C. Gao, X. Xu, Z. Fu, X. Fei, Y. Zhao, Q. Chen, X. Liu, Q. Wei, G. He and H. Fong, *Sol. Energy Mater. Sol. Cells*, 2012, **103**, 53-61.
33. C. Chen, L. Wang and Y. Huang, *Appl. Energy*, 2011, **88**, 3133-3139.
34. C. Chen, L. Wang and Y. Huang, *Chem. Eng. J.*, 2009, **150**, 269-274.
35. C. Chen, L. Wang and Y. Huang, *Mater Lett*, 2009, **63**, 569-571.
36. J. T. McCann, M. Marquez and Y. Xia, *Nano Lett.*, 2006, **6**, 2868-2872.
37. Y. Cai, X. Zong, J. Zhang, Y. Hu, Q. Wei, G. Hei, X. Wang, Y. Zhao and H. Fong, *Sol. Energy Mater. Sol. Cells*, 2013, **109**, 160-168.
38. Y. Cai, H. Ke, L. Lin, X. Fei, Q. Wei, L. Song, Y. Hu and H. Fong, *Energy Convers. Manag.*, 2012, **64**, 245-255.
39. J. T. Korhonen, P. Hiekkataipale, J. Malm, M. Karppinen, O. Ikkala and R. H. A. Ras, *ACS Nano*, 2011, **5**, 1967-1974.
40. B. L. Chen, S. C. Xiang and G. D. Qian, *Accounts Chem Res*, 2010, **43**, 1115-1124.
41. T. Mehling, I. Smirnova, U. Guenther and R. H. H. Neubert, *J Non-cryst Solids*, 2009, **355**, 2472-2479.
42. W. Xia, B. Qiu, D. G. Xia and R. Q. Zou, *Sci Rep*, 2013, **3**, 1935.
43. Z. S. Wu, S. Yang, Y. Sun, K. Parvez, X. Feng and K. Muellen, *J. Am. Chem. Soc.*, 2012, **134**, 9082-9085.
44. S. D. Zhang, M. Zhou, X. Lu, C. Z. Wu, Y. F. Sun and Y. Xie, *Crystengcomm*, 2010, **12**, 3571-3578.
45. S. Zhang, Q. Tao, Z. Wang and Z. Zhang, *J. Mater. Chem.*, 2012, 22, 20166-20169.
46. W. D. Liang, G. D. Zhang, H. X. Sun, Z. Q. Zhu and A. Li, *RSC Adv.*, 2013, **3**, 18022-18027.
47. S. P. Wang, P. Qin, X. M. Fang, Z. G. Zhang, S. F. Wang and X. C. Liu, *Sol. Energy*, 2014, **99**, 283-290.
48. D. D. Mei, B. Zhang, R. C. Liu, Y. T. Zhang and J. D. Liu, *Sol. Energ. Mat. Sol. Cells*, 2011, **95**, 2772-2777.
49. L. Feng, W. Zhao, J. Zheng, S. Frisco, P. Song and X. Li, *Sol. Energy Mater. Sol. Cells*, 2011, **95**, 3550-3556.
50. J. Jiang, Y. Zhu, A. Ma, D. Yang, F. Lu, J. Chen, J. Shi and D. Song, *Progress in Natural Science: Materials International*, 2012, **22**, 440-444.
51. X. Xiao and P. Zhang, *Sol. Energy Mater. Sol. Cells*, 2013, **117**, 451-461.
52. S. Sinha-Ray, R. P. Sahu and A. L. Yarin, *Soft Matter*, 2011, **7**, 8823-8827.
53. L. Chen, R. Zou, W. Xia, Z. Liu, Y. Shang, J. Zhu, Y. Wang, J. Lin, D. Xia and A. Cao, *ACS Nano*, 2012, **6**, 10884-10892.
54. Z. Zhang and X. Fang, *Energy Convers. Manag.*, 2006, **47**, 303-310.
55. L. Xia, P. Zhang and R. Z. Wang, *Carbon*, 2010, **48**, 2538-2548.
56. Y. Zhong, M. Zhou, F. Huang, T. Lin and D. Wan, *Sol. Energy Mater. Sol. Cells*, 2013, **113**, 195-200.
57. H. Ji, D. P. Sellan, M. T. Pettes, X. Kong, J. Ji, L. Shi and R. S. Ruoff, *Energ. Environ. Sci.*, 2014, **7**, 1185-1192.
58. G. Xin, H. Sun, S. M. Scott, T. Yao, F. Lu, D. Shao, T. Hu, G. Wang, G. Ran and J. Lian, *ACS Appl. Mater. Inter.*, 2014, **6**, 15262-15271.
59. T. P. Fellinger, R. J. White, M.-M. Titirici and M. Antonietti, *Adv. Funct. Mater.*, 2012, **22**, 3254-3260.
60. S. A. Al-Muhtaseb and J. A. Ritter, *Adv. Mater.*, 2003, **15**, 101.
61. C. Wang, L. Feng, W. Li, J. Zheng, W. Tian and X. Li, *Sol. Energy Mater. Sol. Cells*, 2012, **105**, 21-26.
62. L. Ventola, M. Ramirez, T. Calvet, X. Solans, M. A. Cuevas-Diarte, P. Negrier, D. Mondieig, J. C. van Miltenburg and H. A. J. Oonk, *Chem. Mater.*, 2002, **14**, 508-517.
63. Z. Liu, R. Zou, Z. Lin, X. Gui, R. Chen, J. Lin, Y. Shang and A. Cao, *Nano Lett.*, 2013, **13**, 4028-4035.

Nanoconfinement of phase change materials within Carbon Aerogels: Phase Transition Behaviours and Photo-to-Thermal Energy Storage

Xinyu Huang, Wei Xia, and Ruqiang Zou *

Department of Materials Science and Engineering, College of Engineering, Peking University, Beijing, P. R. China, 100871

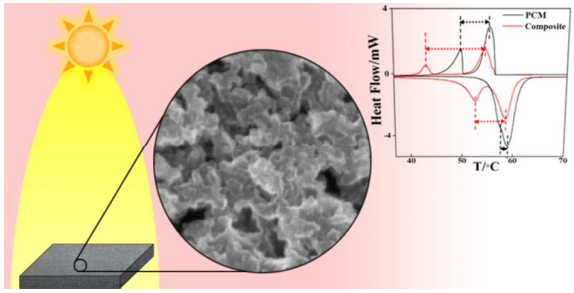

Nanoconfinement of octadecanol within carbon aerogels leads to a novel phase change composites with various phase transition behaviours for photo-to-thermal transformation and storage.